Physics – Uspekhi **41** (6) 595 – 604 (1998)

ON THE 90TH ANNIVERSARY OF L D LANDAU'S BIRTH

PACS numbers: **71.10.–w**, **71.20.–b**, **71.22.+i**, **71.90.+q**

Non-Fermi-liquid metals

L B Ioffe, A J Millis

Contents

Abstract. The experimental discovery of a number of 'strange metals' has reopened the question of the low temperature behavior of interacting Fermi systems. Here we provide a subjective overview of some aspects of the resulting theoretical work. It seems to us that from a theoretical standpoint Landau's Fermi-liquid theory has proven to be a remarkably robust description of clean Fermi systems. The only well documented theoretical examples of non-Fermi-liquid behavior are metals subject to gauge interactions or at quantum critical points. The experimental anomalies which prompted the reexamination of Fermi-liquid theory remain in many cases mysterious.

1. Introduction

Our present-day understanding of metal physics is based on L D Landau's insight that electron-electron interactions are unimportant at low energies. They introduce finite renormalizations and lifetimes vanishing as ω, $T \to 0$, which may be understood perturbatively and do not change the physics qualitatively from that of non-interacting electrons. The past two decades have seen the experimental discovery of a number of 'strange metals' whose behavior is apparently not well described by Fermi-liquid theory. Examples include quasi-one-dimensional organic conductors [1], a two dimensional electron gas in the presence of disorder [2], or magnetic fields [3], some 'heavy fermion' compounds [4] and high temperature superconductors. These experimental discoveries have prompted theorists to reconsider the circumstances under which fermi liquid theory breaks down and what possible 'non-Fermi-liquid' metals might exist. In this article we summarize the progress which has been made in this direction focusing on the behavior of clean systems.

L B Ioffe Physics Department, Rutgers University,
Piscataway, NJ 088855
Tel. (732) 445-46 05. Fax (732) 445-44 00
E-mail: ioffe@physics.rutgers.edu
L D Landau Institute for Theoretical Physics,
Russian Academy of Sciences,
ul. Kosygina 2, 117334 Moscow, Russia
A J Millis Department of Physics and Astronomy
The Johns Hopkins University
3400 North Charles Street,
Baltimore, MD 21218, U.S.A.
Tel. (410) 516-85 86. Fax (410) 516-72 39
E-mail: millis@pha.jhu.edu

Received 5 March 1998
Uspekhi Fizicheskikh Nauk **168** (6) 672 – 682 (1998)
Translated by L B Ioffe

2. Definition of Fermi-liquid theory

The canonical problem which Fermi-liquid theory aims to solve is the behavior of a finite density, n, of electrons, in d spatial dimensions, interacting with each other via a short ranged interaction (because of screening, the Coulomb interaction is effectively short ranged) and with a periodic potential. If the electron-electron interactions are neglected the solution is straightforward in principle: the single-particle Schrödinger equation defines energy bands $\epsilon_n(k)$ which in equilibrium are populated by electrons according to the Fermi – Dirac distribution with chemical potential μ,

$$n_k \equiv n(\epsilon_k) = \frac{1}{\exp[(\epsilon_k - \mu)/T] + 1} \, .$$

One has a metal if at $T = 0$ there is at least one partly filled band. In this case there is a Fermi surface defined by $\epsilon_n(\mathbf{k}) = \mu$; this is a surface in k-space; as one moves across it the k-space conduction-band occupancy n_k drops from 1 to 0. The volume enclosed by the Fermi surface is equal to the density of electrons in the conduction band. The low energy excitations are constructed by removing electrons from filled states near the Fermi surface and adding then to empty states also near the Fermi surface. These excitations are called particle-hole pairs; the particle and hole may be characterized by a crystal momentum $\mathbf{k}$ and an energy $\epsilon_k - \mu \equiv \xi_k = v_k|k - k_F|$. They are eigenstates of the single-particle Schrödinger equation and so have an infinite lifetime.

Landau's fundamental insight was that these qualitative properties also hold for interacting systems because at low energies the available phase space severely restricts possible scattering processes. For example, two electrons initially in states k_1 and k_2 near the fermi surface may only be scattered to final states k_3 and k_4 which are also near the fermi surface; energy and momentum conservation imply that the phase volume of possible final states is proportional to

$$k_{\mathrm{F}}^{d-2}\,\frac{\left(|\xi_{k_1}|+|\xi_{k_2}|\right)^2}{v_{\mathrm{F}}^2}$$

in all $d>1$. Landau's insight may be formalized in at least three ways: Landau's original derivation, which involves writing the energy as a functional of n_k AGD, diagrammatic derivations involving formal resummations of the many-body perturbation theory [5], and renormalization group arguments [6]. All of these methods lead to the same conclusion: the essential features of the non-interacting system are preserved in the interacting one. Specifically, there is a fermi surface *defined* as the locus in k-space across which the occupancy n_k (of the single-particle state of crystal momentum k) has a step. The magnitude of the step is less than 1, and the step may not be located in the same place as in the non-interaction system but the step exists and the k-space volume enclosed by the fermi surface is preserved. Further, although the exact eigenstates are of course very complicated combinations of single-particle states, asymptotically they have a non-zero overlap with single particle states of momentum k and renormalized dispersion $\xi_k^*=v_k^*|k-k_{\mathrm{F}}|$ (where '$*$' denotes renormalized quantities and k_{F} denotes the true Fermi surface of the interacting system). More precisely, the propagation of an injected electron is described by the Green function which may be written (here $\mathbf{T}_t$ is the time-order symbol)

$$G(\omega,k)\equiv\int \mathrm{d}t\exp(\mathrm{i}\omega t)\langle\mathbf{T}_t c_k^{\dagger}(t)c_k(t)\rangle = \frac{Z_k(\omega)}{\omega-\xi_k^*+\mathrm{i}\Gamma_k(\omega)}+G_{\mathrm{inc}}\,.$$

Here G_{inc} is a smooth function of ω and k; the non-smooth (quasiparticle) part is described by a renormalized dispersion ξ_k, a quasiparticle weight $Z_k(\omega)$ and a lifetime $\Gamma_k(\omega)$. If $\Gamma(\omega)=0$ the quasiparticle part describes coherent propagation and Z is the overlap referred to above. The result of the derivations referred to above is that although $\Gamma_k(\omega)$ is non-zero, it vanishes faster than ω, ξ as ω, $\xi\to 0$. This behavior of G may be used to show that the physical content of the theory at low energies includes a specific heat which is asymptotically linear in temperature, a magnetic susceptibility which tends to a constant, and a resistivity which as $T\to 0$ vanishes at least as rapidly as $\Gamma(\omega=0,T)$ (subtleties connected with Umklapp scattering and the dissipation of momentum can make the resistivity vanish faster). In the usual fermi liquid in $d=3$ $\Gamma(T)$ is of the order of T^2; in $d=2$, $\Gamma(T)\sim T^2\ln T$. Experimentalists tend to define non-fermi-liquid behavior as a specific heat which vanishes less rapidly than T or a resistivity which vanishes less rapidly than T^2. The well known T-linear resistivity of high T_{c} superconductors has encouraged the belief that these materials are not fermi-liquids.

A more theoretical definition of non-fermi-liquid behavior seems desirable. We distinguish strong and weak versions of non-fermi-liquid behavior. In a strong non-fermi-liquid the electron Green function is smooth everywhere; there is no singularity which could be used to define a fermi surface. The only examples known at $T=0$ are band insulators, which are trivial, superconductors and spin or charge density wave systems, where due to a phase transition to an ordered state a gap opens up in the electronic spectrum. In a weak non-fermi-liquid the Green function and hence the single particle occupancy n_k has a singularity (albeit perhaps not a step) which defines the fermi surface, but the relaxation rate vanishes less rapidly than ω as $\omega\to 0$. Several theoretical models of weak non-fermi-liquids exist, including the $d=1$ Luttinger liquid, certain quantum critical points in two and three dimensions, and electrons coupled to a gauge field in two or three dimensions. The T-linear resistivity of high T_{c} superconductors led to the proposal of a 'marginal fermi liquid' in which $\Gamma\sim\omega$.

Weak or strong non-fermi-liquid behavior can only occur if the assumptions underlying the conventional derivations of fermi liquid theory break down. The theoretical status of conventional fermi liquid theory is as follows: for weak short-ranged interactions it may be derived by perturbation theory, which is apparently well behaved in sufficiently high dimension. In $d=3$ the perturbative results have never been questioned. In $d=2$ doubts have been raised about even the leading order result [7] or about singularities arising on resummation to infinite order [8], but other work [9, 10] has shown that perturbation theory is well behaved even in $d=2$. Additionally, diagrammatic resummation and renormalization group analysis [6] have shown that if this behavior is assumed at some energy scale $\epsilon_0\ll\epsilon_{\mathrm{F}}$ then it persists down to $\epsilon=0$, i.e. the Fermi liquid is a stable fixed point in the renormalization group sense, in $d=2$ and $d=3$. Therefore, obtaining a non-fermi-liquid metal requires low dimensionality ($d=1$ or $d=0$, i.e impurity models), an interaction stronger than some critical value or a generalized model including a singular interaction or disorder or high magnetic fields. The physics of impurity models and 1d metals, the physics of high magnetic fields [3] and the physics of disordered metals [2] have been discussed at length elsewhere and will not be considered further here (except for the $\nu=1/2$ quantized Hall state). Concerning strong interactions two cases arise: one is that at a particular critical interaction strength a $T=0$ second order phase transition occurs. The critical fluctuations associated with this phase transition lead to a singular interaction incompatible with the assumptions used in deriving fermi liquid theory and thus to non-fermi-liquid behavior at the critical point. This will be discussed in Part 3. The second is that there is a range of strong couplings leading to non-fermi liquid metallic behavior. No model is known which gives rise to such behavior down to $T=0$, although to our knowledge there is no proof that such a model cannot exist. Several models, motivated by the properties of high T_{c} superconductors, exhibit non-fermi liquid behavior over a wide range of temperatures, but all of them cross over to Fermi-liquid behavior at sufficiently low T. These will be discussed in part 4.

3. Quantum critical phenomena and non-Fermi-liquid physics (ferromagnets)

At a second order $T=0$ phase transition (the quantum critical point) fluctuations of the order parameter have long ranged (power law) correlations in space and time. The

density of states corresponding to these fluctuations may be constant or even divergent at low energies (in contrast to a non-critical Fermi liquid), so scattering of electrons off them may lead to weak non-fermi-liquid behavior.

To give some flavor of these calculations we consider the electron Green function near the ferromagnetic quantum critical point of a 2D or 3D fermi liquid in some detail. Experimental realizations of three dimensional transitions include MnSi [11], $ZrZn_2$ [12] and $TiBe_2$ which are all 'weak ferromagnets' in which the Curie temperature may be tuned to 0 by hydrostatic pressure. These transitions have been extensively studied by the usual techniques of critical phenomena which involve integrating out all non-critical degrees of freedom including conduction electrons, obtaining an action describing the long wavelength magnetization fluctuations and analyzing this action. It was found by Hertz [13, 14] that the long wavelength spin fluctuations are described by the propagator

$$D(\omega, q) = \left[\frac{p_0|\omega|}{2\pi q} + Dq^2 + \xi^{-2}(T)\right]^{-1}, \tag{1}$$

where ξ is the correlation length which diverges at the critical point, p_0 is the scale of order of Fermi momentum and D is the spin stiffness. The spin fluctuation propagator (1) can be written in terms of the two-particle irreducible bubble $\Pi(\omega, q)$ and an interaction vertex U as $D = 1/(D_0^{-1} - U\Pi)$. For non-interacting fermions $\Pi(0, q)$ is an analytic function of q^2 and it is usually assumed that $\Pi(0, q)$ and U remain analytic functions of q^2 even when short range interactions are taken into account, so that at the critical point $D^{-1}(0, q) \propto q^2$. However this belief was recently called in to question by calculations yielding $q^2 \ln q$ in three dimensions and $|q|$ in two dimensions [15]. If correct, this would make the quantitative results derived below inapplicable, but the method of analysis and the qualitative conclusions (such as the smallness of the vertex corrections) would not change. In any case, because the spin system is embedded in a fermi liquid, the spin dynamics is overdamped; the specific form $|\omega|/q$ in (1) comes from the familiar Landau damping.

Equation (1) is the result of the mean field theory; however mean field theory has been shown to give asymptotically correct behavior for this problem. The essence of the argument is this. Equation (1) implies the dynamical exponent $z = 3$ because one power of the frequency scales as three powers of momentum. Because the spin wave interactions (i.e. ϕ^4 terms) have non-divergent coefficients, the effective dimensionality of the critical theory $d_{\text{eff}} = d + z$; thus in both $d = 2$ and $d = 3$, $d_{\text{eff}} > 4$ so the theory is above the upper critical dimension and its properties may be studied by perturbation theory. Two results relevant to the present discussion are (i) if the parameters (such as pressure) are tuned so that at $T = 0$ the system is at the critical point, $\xi^{-2}(T) \sim T^{4/3}$ in $d = 3$ and $\xi^{-2}(T) \sim T/\ln T$ in $d = 2$, much less than the characteristic scale $T^{2/3}$ of q^2 or $|\omega|/q$ for typical $\omega \sim T$ and (ii) the specific heat is of the order $T \ln T$ in $d = 3$ and $T^{2/3}$ in $d = 2$ [14]. The behavior of the specific heat is non-fermi-liquid in the empirical sense discussed in the previous section.

We now consider the behavior of the single particle Green function in this non-fermi-liquid using diagrammatic arguments adopted from [16]. The leading order diagram for the self energy is shown in part (a) of Fig 1. This diagram may be evaluated using a non-interacting fermion Green function $G^{-1} = (\omega - v|k - k_F|)$ and the spin fluctuation propagator given by (1). The result is

$$\Sigma^{(1)}(\omega) = \frac{3}{8\pi^2}\frac{v_F p_0}{p_F^2 D}\left[\epsilon \ln\left(\frac{E_F}{\epsilon}\right) + i\frac{\pi}{2}\epsilon\right] \tag{2}$$

for $d = 3$ and

$$\Sigma^{(1)} \sim \epsilon\left(\frac{\omega_0}{\epsilon}\right)^{1-d/3}$$

in $d < 3$ with ω_0 an energy scale of the order of E_F. Thus the leading approximation to the theory is a weak ($d < 3$) or marginal ($d = 3$) non-fermi-liquid; the physical consequences include a specific heat which varies as $T^{d/3}$ ($T \ln T_0/T$ in $d = 3$) and an n_k which has a cusp at k_F rather than a jump. Note that in this approximation the non-analytic part of the self energy is a function of energy only.

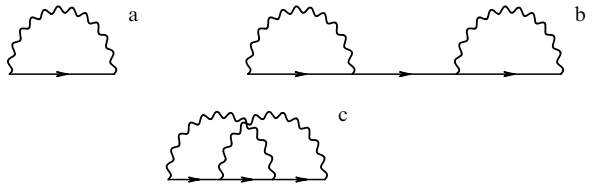

Figure 1. Fermion self energy diagrams. The wavy line denotes the fluctuation propagator (1) and the solid line the fermion propagator.

We now discuss higher order corrections, such as those shown in Fig. 1b, c. Those shown in Fig. 1b scale as $\Sigma^{(b)} \sim [\Sigma^{(1)}(\epsilon)]^2/\epsilon$ while direct calculation gives $\Sigma^{(c)} \sim \epsilon^{2/3(d-2)}\epsilon$. These can also be seen to be small by the arguments underlying the Migdal theory of electron-phonon interaction. These arguments are that the energy transferred in an electron-phonon scattering process is small, so all intermediate states must be near the Fermi surface, and that the curvature of the fermi surface severely restricts the phase volume available for interference processes so these processes are weak and can be ignored. Clearly for these arguments to apply the curvature term in the electron dispersion should be important for a process involving a typical momentum transfer. The same logic applies here. To see this quantitatively note that the electron Green function can be written as

$$G(\epsilon, p) = \left[\epsilon - \Sigma_p(\epsilon) - v\left(p_\parallel + \frac{p_\perp^2}{2p_0}\right)\right]^{-1}. \tag{3}$$

Here we have separated the momentum into components parallel and perpendicular to v_F (cf. Fig. 4) and have introduced the fermi surface curvature p_0^{-1}. In a typical process involving an energy transfer ω, the momentum transferred, $k_\omega \sim \omega^{1/3}$ so the curvature term scales as $\omega^{2/3}$. For $d > 2$ this is more important than the self energy (which scales as $\omega^{d/3}$) and so is relevant. As usual the effect of this term is to decrease the effect of interference terms. The result is the Migdal theory with an expansion parameter $(\omega/E_F)^{(d-2)/3}$. One consequence of this theory is that the leading order diagram gives an asymptotically exact expression for the self energy. In the terminology of critical phenomena, the singular contribution to the self energy is described by a scaling function which depends on frequency

only, involves the exponent $d/3$ and because of the Gaussian nature of the theory may be computed exactly. Note also that the crucial scattering processes are those which move the electrons along the Fermi surface and that the non-analyticities in the fermion propagator do not feed back and change the form of the spin fluctuation propagator which is always given by Eqn (1).

The case of $d = 2$ is more subtle. The Migdal arguments show that the leading self-energy scales in the same way ($\omega^{2/3}$) as the $k_\perp$ dependence; the vertex corrections are therefore marginal and a more complicated treatment of the electron problem is required. Note however that the critical theory is still above its upper critical dimension, so the spin propagator is still given by Eqn (1).To study the electron propagator an expansion parameter is required; the analogy to the Migdal theory motivated us to introduce one which controls the relative importance of scattering parallel and perpendicular to the Fermi surface. Paper [16] did this for the gauge interaction problem; the treatment carries over with only minor modifications to the ferromagnetic case. We introduce the parameter N via

$$D_N(\omega, q) = \left(N \frac{p_0|\omega|}{2\pi q} + \frac{1}{\sqrt{N}} q^2 \right)^{-1}, \tag{4}$$

so that a typical momentum transfer is $k_\omega \sim \sqrt{N}\omega^{1/3}$; we have chosen this precise form (involving the choice of energy units so that $D = 1/\sqrt{N}$), so that the first order self energy is independent of N. Because $k_\omega \sim N^{1/2}\omega^{1/3}$ for large N the curvature term,

$$\frac{k_\omega^2}{p_0} \sim N\omega^{2/3} \gg \Sigma^{(1)}(\omega)\,,$$

becomes important and a Migdal approximation can be constructed with the expansion parameter $1/N$. Therefore at large N the leading order is

$$G^{(2D)} = \frac{1}{\omega_0^{1/3}\epsilon^{2/3} - v|p_\parallel - p_\mathrm{F}|}\,, \tag{5}$$

where $\omega_0 = (1/2\sqrt{3})^3(2/\pi^2)$ is a numerical coefficient.

Explicit calculation shows that the next order correction turns out to be of order $\sim (\ln N/4\pi N)^2\Sigma^{(1)}$; the $\epsilon^{2/3}$ is thus preserved. The self energy acquires a p-dependence which has not been studied in detail. At small $N k_\omega^2/p_0 \ll \Sigma^{(1)}(\omega)$ and all higher order terms are equally important. Strictly in the limit $N \to 0$ one can neglect the effects of electron displacement along the Fermi surface on the electron Green function, so the electron scattering becomes essentially one dimensional. Therefore in this limit we may treat each ray in the momentum space of electrons as an independent one dimensional system and study it by bosonisation. We find that in the limit of low energy and momenta close to the Fermi surface $G(\mathbf{p}, \epsilon)$ acquires a simpler scaling form

$$G^{(1D)}(\epsilon, p) = \frac{-1}{v_\mathrm{F}(p - p_\mathrm{F})} g\left(\frac{\Gamma(2/3) l_0^{-1/3}\epsilon^{2/3}}{v_\mathrm{F}^{2/3}(p - p_\mathrm{F})} \right),$$

$$g(u) = \frac{3}{2}\exp\left[(-1)^{3/4}u^{3/2}\right] - \frac{3\sqrt{3}\mathrm{i}}{4\pi}\int_0^\infty \frac{\exp\left[-(uy)^{3/2}\right]\mathrm{d}y}{y^2 + \mathrm{i}y - 1}\,. \tag{6}$$

Although the Green functions (6) and (5) have completely different analytical structures, their qualitative properties are similar: both are equal to $1/v_\mathrm{F}|p_\mathrm{F} - p|$ in the limit $\omega_0^{1/3}|\epsilon|^{2/3} \ll v|p - p_\mathrm{F}|$ and both behave as $1/(\omega_0^{1/3}|\epsilon|^{2/3})$ in the opposite limit $\omega_0^{1/3}|\epsilon|^{2/3} \gg v|p - p_\mathrm{F}|$. We therefore expect a smooth crossover from formula (6) to (5) as $N \to 0$. Both describe overdamped fermions with a characteristic energy that scales as $(p - p_\mathrm{F})^{3/2}$. Thus, the limit $N \to 0$ is not singular for the fermion Green function. Our derivation suggests that the precise form [given in Eq (6)] depends on two special 'one-dimensional' features: the neglect of internal loops and the neglect of the perpendicular momentum in fermion propagators. Both these features are present in the $N \to 0$ limit but are not present at arbitrary N. For this reason we do not believe that the exponential form is generic, although the correspondence between the $N \to 0$ and $N \to \infty$ limits lead us to believe that the scaling $\epsilon^{2/3} \propto p_\parallel$ is.

A non-zero N leads to coupling between different points on the Fermi surface; the problem is then not strictly one dimensional. Small but nonzero N may be studied by Ward identity techniques. The result is, as expected, that the scaling $\epsilon^{2/3} \propto p_\parallel$ is preserved but the form of G is changed qualitatively from the one dimensional form given in Eqn (6). This is of theoretical interest because several authors have argued that bosonisation techniques may be applied to a two dimensional electron gas [17, 18]. In the singular interaction case of interest here, these techniques produce a G precisely of the form of Eqn (6) above. However, we have seen that this form is correct only when scattering along the Fermi surface is completely neglected ($N \to 0$), suggesting that the bosonisation method does not adequately treat these processes. It is instructive to generalize the previous analysis to the case of electrons in d spatial dimensions interacting with the overdamped bosonic mode with propagator $D = 1/(|\omega|/q + q^x)$. If $d > 2$ and $x > d - 1$, the result is weak 'Migdal' non-fermi-liquid behavior characterized by a self energy $\Sigma(\omega) \sim \omega^{d/(x+1)}$ with a singular dependence only on the frequency and corrections of order $\omega^{(d-2)/(x+1)}$ to the leading behavior; in $d = 2$ one also obtains a weak non-fermi-liquid but now Σ is function of both ω and $p_\parallel$.

So far we have discussed the effects of critical fluctuations on the electron self energy. The vertices connecting electrons to small momentum transfer spin fluctuations are not renormalized, essentially because the spin theory is above its critical dimension. Now we turn to the renormalization of the fermion vertices with large momentum transfer. The corrections to the vertex with large but arbitrary momentum transfer $|\mathbf{q}| \sim p_\mathrm{F}$ are generally small because of the small phase volume available for virtual processes which leave both fermions with momentum transfer $\mathbf{p} + \mathbf{q} + \mathbf{k}$ and $\mathbf{p} + \mathbf{k}$ close to the Fermi surface. The situation changes only for $|q|$ close to $2p_\mathrm{F}$. In this case a virtual process with momentum transfer $\mathbf{q}$ along the Fermi surface leaves both fermions with momenta $\mathbf{p} + \mathbf{q} + \mathbf{k}$ and $\mathbf{p} + \mathbf{k}$ near the Fermi surface.

In three dimensions this leads to only subleading effects but in two dimensions the leading contribution in $1/N$ to the fermion vertex Γ_Q is logarithmically divergent at $Q = 2p_\mathrm{F}$; we find that higher powers of N contain higher powers of logarithms; we sum these logarithms using a renormalization group method and find power law singularities in Γ_{2p_F}. These singularities imply that the calculation of the particle-hole susceptibility must be reconsidered. Finally, a singular susceptibility near $2p_\mathrm{F}$ may be further modified by the short range four fermion interaction; therefore we must also consider the renormalization of this interaction by the critical fluctuations.

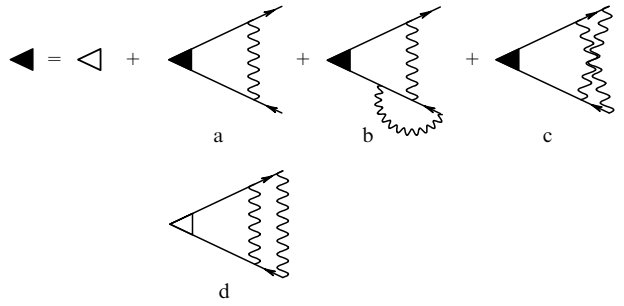

Figure 2. Diagrams giving the renormalization of fermion vertex Γ_{2p_F} (shaded triangle). (a) Leading order in $\ln(\omega)/N$, (b) and (c) subleading order in 1/N, (d) leading order in $[\ln(\omega)/N]^2$. Wavy line denotes critical fluctuations (1), solid line the fermion propagator.

We begin with the diagrams for Γ_Q shown in Fig. 2a. The diagrams shown there diverge logarithmically if all external momenta are on the Fermi surface, the external energies are zero and the momentum transfer is exactly $Q = 2p_F$. Since the energy only enters the Green function via $\omega_0^{1/3}|\epsilon|^{2/3}$, the momentum component across the Fermi surface via $v_F k_\parallel$ and the momentum along the Fermi surface via $k_\perp^2$, the divergence is cut off by the largest among

$$\epsilon,\ \epsilon_\parallel = \frac{(v_F k_\parallel)^{3/2}}{\omega_0^{1/2}},\ \epsilon_\perp = \frac{k_\perp^3/m^{3/2}}{\omega_0^{1/2}}\,. \tag{7}$$

If, say, the largest is the external frequency we evaluate the diagrams in Fig. 2 and get

$$\delta\Gamma_{2p_F}(\omega) = \pm\left[\frac{1}{2N} + \frac{1}{2\pi^2 N^2}\ln^3(N)\right]\ln\left(\frac{1}{\omega}\right)\Gamma^0_{2p_F}\,, \tag{8}$$

where $\Gamma^0_{p_F}$ is the bare vertex at small scales or large frequencies. The sign '+' in (8) corresponds to the spin density vertex while the sign '−' corresponds to charge density. The logarithmic nature of the corrections to the effective interaction allows us to sum higher orders of the perturbation theory by constructing the renormalization group equation:

$$\frac{\mathrm{d}\Gamma_{2p_F}}{\mathrm{d}\ln(1/\omega)} = \left[\frac{1}{2N} + \frac{1}{2\pi^2 N^2}\ln^3(N)\right]\Gamma_{2p_F}\,. \tag{9}$$

From (9) we see that the vertex grows at large scales as

$$\Gamma^R_{2p_F} \sim \left(\frac{\epsilon_F}{\omega}\right)^{\sigma}\Gamma^0_{2p_F}\,, \tag{10}$$

$$\sigma = \frac{1}{2N} + \frac{1}{2\pi^2 N^2}\ln^3(N) + O\left(\frac{1}{N^2}\right). \tag{11}$$

Here we used the energy ω for the infra-red cut off assuming that it sets the largest scale among $\omega, \epsilon, \epsilon_\parallel, \epsilon_\perp$. The result (10) is derived using a large N expansion. It is also of interest to evaluate these diagrams at $N = 2$. The leading order diagram gives $\sigma = 0.25$; the sum of the diagrams shown in Fig. 2b and 2d gives $\sigma = 0.35$.

The power law growth of the vertex at $2p_F$ distinguishes fermions at the quantum critical point from an ordinary Fermi liquid with short range repulsion and leads to anomalous behavior of the spin correlators at $Q = 2p_F$. In the absence of a short range interaction effective at $2p_F$ the spin correlator is given by the polarization diagrams shown in Fig. 3. The leading contributions in powers of $(1/N)\ln\omega$ come from the diagrams in which the vertical lines of the fluctuations do not cross. In these diagrams the leading contribution originates from the frequency range (and the corresponding momentum range, which we have not explicitly written)

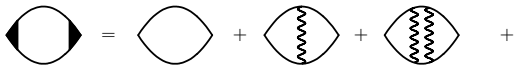

Figure 3. Ladder sums giving the renormalization of fermion $2p_F$ polarizability. The notation is the same as in Figs 1, 2

$$\epsilon_F > \omega_n > \ldots \omega_1 > \omega < \ldots < \omega_{-n} < \epsilon_F\,,$$

where ω is the external frequency. Therefore, the sum of all diagrams is given by the diagram shown in Fig. 3 with renormalized vertices ($\Gamma^R_{2p_F}$):

$$\Pi(\omega, q) = \int G\left(\epsilon + \frac{\omega}{2}\,,\ p + \frac{q}{2}\right)G\left(\epsilon - \frac{\omega}{2}\,,\ p - \frac{q}{2}\right) \times \left[\Gamma^{(R)}_{\epsilon,p}(\omega, q)\right]^2 \mathrm{d}p\,\mathrm{d}\epsilon\,. \tag{12}$$

To evaluate the integral in (12) we note that the main contribution comes from the range of momenta and energies related by $\epsilon \sim \epsilon_\parallel \sim \epsilon_\perp \sim \omega$ [see (7)]. Estimating the result by power counting we find that if $\sigma < 1/3$ (as occurs for large N) integral (12) converges, but if $\sigma > 1/3$ it diverges at $\omega = 0$, $q = 2p_F$. We evaluate the integral in these cases separately and find:

$$\Pi(\omega, q) = \Pi_0 - \sqrt{\frac{p_0}{\omega_0 v_F^3}}\left[c_\omega\left(\frac{\omega}{\omega_0}\right)^{2/3-2\sigma} + c_q\left(|q - 2p_F|l_0\right)^{1-3\sigma}\right],\quad \sigma < 1/3\,, \tag{13}$$

$$\Pi(\omega, q) = \sqrt{\frac{p_0}{\omega_0 v_F^3}}\left[c_\omega\left(\frac{\omega}{\omega_0}\right)^{2\sigma-2/3} + c_q\left(|q - 2p_F|l_0\right)^{3\sigma-1}\right]^{-1},\quad \sigma > 1/3\,, \tag{14}$$

where the coefficients c_q and c_ω are of the order of unity for a curved Fermi surface. Below we shall assume that $c_q = c_\omega = 1$. Since these coefficients depend strongly on the curvature of the Fermi surface, the case of a flat Fermi surface should be considered separately. We shall not discuss it further here.

Note that the strong singularity of the correlators at momentum transfer $2p_F$ discussed above is special to two dimensions. In higher dimensions the leading correction to Γ_Q vertex remains finite (albeit non-analytical) even at momentum transfer $2p_F$ and does not lead to any interesting physical effects.

4. Other non-Fermi-liquids

4.1 Electrons interacting with magnetic field fluctuations

As noted by Holstein [19] and Reizer [20] a moving electron makes a magnetic field which will affect the motion of other

electrons. If the magnetic field is represented by a vector potential and the effect of Landau damping is included, the resulting problem is very similar to a critical ferromagnet but with $\xi^{-1} = 0$ at all T. The effects however are small by two powers of the fine structure constant $\alpha \approx 1/137$.

It was argued that a similar two dimensional gauge field theory describes relevant excitations of the half filled Landau level [21, 22]. These arguments relied on a singular gauge transformation that eliminates the average magnetic field at the expense of introducing a fluctuating gauge field. Qualitatively this gauge transformation can be understood as the attachment of a flux tube carrying flux $\Phi = 2\Phi_0$ (where $\Phi_0 = hc/e$ is flux quantum) of fictitious magnetic field to each electron. The important point is that such an attachment cancels the average external magnetic field and brings about an additional phase $\exp(2i\theta_{ij})$ for each pair of electrons and therefore does not make their wavefunction multivalued [rotation of one electron around another brings $\exp(4i\pi) = 1$] and does not change the electron statistics because interchanging electrons is equivalent to rotation by π [which brings a factor $\exp(2i\pi) = 1$] and translation. From this construction it is clear that the fluctuations of the fictitious magnetic field are coupled to the fluctuations of the density of the electron gas. Therefore the Coulomb interaction which suppresses the fluctuations of the density effectively suppresses these fluctuations as well. In an isolated 2D electron gas the Coulomb interaction is proportional to $1/|k|$ but in fabricated structures the electron gas might be near a metallic gate; in this case the Coulomb interaction is screened on the scale of $\varkappa^{-1}$. The resulting gauge field propagator describing the singular interaction between electrons is [21]

$$D_{\nu=1/2}(\omega, q) = \left(\frac{p_0|\omega|}{2\pi|k|} + \frac{uk^2}{k+\varkappa}\right)^{-1}. \tag{15}$$

Here $u = e^2/8\pi\hat{\epsilon}$ and the appearance of the $1/(8\pi)$ instead of the conventional 2π may be traced to a $1/(4\pi)$ in the coefficient of the Chern–Simons term [21]. Clearly (15) is much less infra-red singular than the propagator of the critical fluctuations (1) and leads to a much weaker effects.

In this subsection we treat the case $\varkappa = 0$; we expect the results to apply if the momenta of interest k'_ω are greater than $\varkappa$. In the other limit, one expects the same results as for critical ferromagnetic fluctuations at $N = 1$. The momenta k'_ω are those for which the two terms in the denominator of (15) are comparable. At temperature T, typical frequencies are $\omega = 2\pi T$ and, if $\varkappa = 0$, we find that typical momenta $k'_T \sim (8\pi p_0 k_B T\hat{\epsilon}/e^2)^{1/2}$. Using a typical Fermi momentum for Ga–Al–As system $p_0 = (4\pi n)^{1/2} \approx 8 \times 10^5$ cm^{-1} and a typical $\hat{\epsilon} = 13$ we find that the unscreened results apply if

$$\varkappa\ [\mathrm{cm}^{-1}] < 4 \times 10^5 T^{1/2}\ [\mathrm{K}]. \tag{16}$$

Thus if at $T = 0.1$ K the screening layer is further than 1000 A from the 2d electron gas, the unscreened results apply. If it is much closer, then one should use the results of the previous section interpolated to $N = 1$.

We turn now to computations using $\widetilde{D}$ (15) with $\varkappa = 0$. The leading order self energy (Fig. 1a) is in $d = 2$

$$\Sigma^{(1)}(\epsilon) = -i\frac{2\hat{\epsilon}v_F}{\pi e^2}\ln\left(\frac{\epsilon_F}{|\epsilon|}\right)\epsilon + \ldots \tag{17}$$

Here the ellipsis indicates terms which are less singular as $\epsilon \to 0$. Arguments identical to those of Section 2 show that $\Sigma^{(1)}$ also solves the leading order Eliashberg equation, so it sums correctly all the rainbow graphs.

We now argue that higher order crossed diagrams give fewer singular contributions to $\Sigma(\epsilon, p)$, so that the leading dependence is given exactly by (17). Consider the leading crossed diagram, Fig. 1c, with the fermion propagators dressed by the self energy (17). After integration over parallel momenta and symmetrization in $q_{\perp 1}$, $q_{\perp 2}$ one finds

$$\Sigma^{(2)}(\epsilon) = v_F^2 \sum_{\omega_1,\omega_2}{}' \int \frac{dk_1}{(p_0|\omega_1|)/(2\pi|k_1|) + u|k_1|} \times \frac{dk_2}{(p_0|\omega_2|)/(2\pi|k_2|) + u|k_2|} \frac{A}{A^2 + (v_F/p_0)k_1k_2}, \tag{18}$$

with

$$A(\omega_1, \omega_2, p_\parallel) = v_F p_\parallel + \Sigma^{(1)}(\epsilon + \omega_1 + \omega_2) + \Sigma^{(1)}(\epsilon + \omega_1) + \Sigma^{(1)}(\epsilon + \omega_2).$$

The prime on $\sum_{\omega_1,\omega_2}$ denotes the constraint that the sum over frequencies is restricted to the region where $\omega_1 + \omega_2 + \epsilon$ has a sign opposite to $\omega_1 + \epsilon$ and $\omega_2 + \epsilon$. This constraint implies that ω_1 and ω_2 cannot vanish simultaneously, so no infra-red singularities arise from the frequency integrals. To extract the infra-red behavior of (18) we may replace A by its typical value $\epsilon \ln(\epsilon_F/\epsilon)$ and $\omega_{1,2}$ by their typical values ϵ. The sum over frequency gives a factor of ϵ^2. The main contribution to the integrals over k_1, k_2 is a logarithmic divergence coming from the region $\epsilon < q^2 < \epsilon \ln \epsilon$; the final result is

$$\Sigma^{(2)}(\epsilon) = \frac{\hat{\epsilon}v_F}{e^2}\epsilon\frac{\ln^2\ln(\epsilon_F/\epsilon)}{\ln(\epsilon_F/\epsilon)}. \tag{19}$$

This is smaller than the leading term by the factor $\{[\ln\ln(\epsilon_F/\epsilon)]/[\ln(\epsilon_F/\epsilon)]\}^2$.

Similar considerations apply to higher order crossed graphs.

This result, that the leading behavior at small frequencies is given exactly by the first order diagram, is again reminiscent of the Migdal theorem, which states that the leading low-frequency behavior of the electron self-energy in the electron-phonon problem is given exactly by the leading order diagram. In the calculations leading to Eqn (17) the energy transferred by the gauge field is small, while the integral over momenta is logarithmic and only cut off at the scale p_F. In the quantum critical case discussed in the previous section, the momentum integrals were confined to the region of small momenta. The problem simplified only in the large N limit where the range of the momentum integration became large in N. Thus, the problem of the half-filled Landau level is analogous to the large N limit of the quantum critical $d = 2$ case.

We now turn to polarization bubbles and vertices. As in the previously considered spin liquid case, the only singularities occur in the $2p_F$ vertices. The leading $2p_F$ vertex correction, Fig. 2a, is given after summing over parallel momenta by

$$\Gamma^{(1)}_{2p_F} = v_F \sum_\epsilon \int dk \left(\frac{p_0|\epsilon|}{2\pi|k|} + \frac{e^2}{8\pi\hat{\epsilon}}|k|\right)^{-1} \times \left(\frac{2\hat{\epsilon}v_F}{\pi e^2}|\epsilon|\ln\epsilon + \frac{v_F}{p_0}k^2\right)^{-1}. \tag{20}$$

Again, the leading contribution to the integral over $k_\perp$ is a logarithm coming from the region $\epsilon < v_F k_\perp^2/p_0 < \epsilon \ln \epsilon$. Performing this integral and evaluating the sum over frequencies we get

$$\Gamma^{(1)}_{2p_F} = \frac{1}{2}\ln^2\left[\ln\left(\frac{\epsilon_F}{\max[T,\omega,v_F(Q-2p_F)^2/p_0]}\right)\right]. \quad (21)$$

Although it is of only academic interest, we note that the higher order corrections may be summed to obtain the leading singular behavior. As in the case of the self-energy, the crossed graphs are less singular than ladder ones. As in Section 2, the sum of the ladder graphs exponentiates, leading to

$$\Gamma_{2p_F} = \exp\left\{\frac{1}{2}\ln^2\left[\ln\left(\frac{\epsilon_F}{T}\right)\right]\right\}. \quad (22)$$

This weak singularity implies that the polarizability is not singular, but the leading frequency and momentum dependence is weakly singular.

4.2 Quantum critical antiferromagnets

Quantum critical antiferromagnets present a related set of issues, but the kinematics of scattering off antiferromagnetic fluctuations differs in a crucial way from that of scattering off ferromagnetic spin fluctuations. In a material near an antiferromagnetic instability the spin fluctuation propagator peaks at some large momentum transfer, **Q**, so most points on the Fermi surface are not connected to other low energy states by spin fluctuation scattering. Three cases are possible:

(1) The generic case: the tangent planes (or lines in $d = 2$) at **p** and **p** + **Q** are not parallel as in the case of points **p** and **p** + **Q** in Fig. 4.

(2) The parallel tangents ('$2p_F$') case: the tangent planes at **p** and **p** + **Q** are parallel as in the case of points **p** and **p** + **Q**′ in Fig. 4 or in the case of points lying opposite to each other on a spherical Fermi surface. In this case the singularities associated with $2p_F$ scattering in the usual Fermi liquid change the picture dramatically

(3) The spin fluctuation scatterings do not connect any points on the Fermi surface (or line). In this case the fermions produce only analytic corrections to the properties of the spin fluctuations and vice versa and the two subsystems can be regarded as effectively independent. We shall not discuss this case here.

4.2.1 Generic case. In this case only at 'hot spots' (in $d = 2$) or 'hot lines' (in $d = 3$) does the fermion self energy acquire a singular frequency dependence, $\Sigma \sim \omega \ln 1/\omega$ in $d = 3$ and $\Sigma \sim \sqrt{\omega}$ in $d = 2$, as one moves away from the hot spots or lines the self energy goes back to the usual Fermi-liquid form. Because only a small portion of the Fermi surface is significantly affected by the critical scattering the singular behavior in e.g. the specific heat should be weaker than for ferromagnets. For example, the theoretical prediction for the leading singular behavior of the specific heat in typical three dimensional antiferromagnet is $T^{3/2}$; in contrast to the $T \ln 1/T$ found for a ferromagnet. This result can be understood as follows. Consider the effective long wave action of spin fluctuations after fermions are integrated out. The main effects of the fermions on this action is the appearance of the dissipative term in the spin fluctuation propagator which becomes

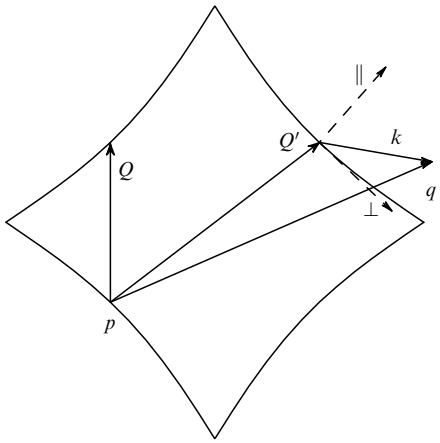

Figure 4. Sketch of Fermi surface and important wave vectors. The fermi line shown here is similar to that found by photoemission spectroscopy in high T_c cuprates. The ordering wave vector **Q** connects two points with parallel tangents, the vector **Q**′ does not. We also show a typical momentum of a spin fluctuation, q, and a local coordinate system convenient for the discussion of fermion processes near the fermi surface.

$$D_{AF}(\omega,q) = \frac{1}{|\omega| + D'|\mathbf{q}-\mathbf{Q}|^2}. \quad (23)$$

The typical frequency of these fluctuations scales as $A|\mathbf{q}-\mathbf{Q}|^2$, giving a density of states $v_{AF} \sim \omega^{1/2}$, such a density of states leads to the specific heat $C \sim T^{3/2}$. This can also be understood in the electron language: in a strip of width $T^{1/2}$ about the 'hot line' the electron self energy is modified by a large factor. Similarly the scattering rate is large near the hot spot, however it only weakly affects the transport properties because these electrons are short circuited by the intact electrons away from the hot spots [24]. Similarly one finds that the Neel temperature scales with pressure as $T_N \sim (p - p_c)^{2/3}$.

The theoretical status of these results is based on the same arguments as in the ferromagnetic case treated above: the spin fluctuations may be shown to be above the upper critical dimension and hence to be described by a gaussian model with the propagator given in Eqn (23). Interaction effects may be computed perturbatively. Experiments on quantum critical antiferromagnets, however, disagree strongly with these theoretical predictions (unlike ferromagnets where experiment and theory agree). Several antiferromagnetic quantum critical systems are known; in all cases $C \sim T \ln T$ and $T_N \sim (p - p_c)$ [25]. The origin of this disagreement is an important open problem.

4.2.2 Parallel tangents ('$2p_F$') case. If the antiferromagnetic wavevector **Q** connects two points on the Fermi surface with parallel tangents, then the scattering kinematics is more complicated and the analysis of the previous section must be modified. In $d = 3$ it turns out that the susceptibility can not have a maximum at such a wavevector, so this case does not arise. In $d = 2$ the spin fluctuation propagator becomes [26]

$$D(\omega,\mathbf{q}) = \frac{2\pi}{N\left[\mathrm{Re}\sqrt{k_\parallel + (k_\perp^2/4) + i\omega} - b(k_\parallel - k_\perp^2/4) + \Delta\right]}. \quad (24)$$

Here a square root singularity is due to a singular electron contribution at $2p_F$. This singular behavior is a consequence of a large phase volume for scattering across the Fermi line and implies that the critical fluctuations have a strong effect on the electrons; furthermore, the $2p_F$ singularities in electron response functions mean that electrons near the Fermi line which are strongly affected by critical scattering have a large effect on the critical fluctuations. We showed that generally it leads to a fluctuation driven first order transition but there is one special case where the transition is not first order. Namely, if twice the ordering vector $\mathbf{Q}$ is commensurate with a reciprocal lattice vector, $\mathbf{G}$, i.e. $2\mathbf{Q} = \mathbf{G}$, then the spin fluctuation propagator is less singular, the fluctuations are weaker and the transition turns out to be second order and characterized by the exponents which we calculate in a $1/N$ expansion. If $|2\mathbf{Q} - \mathbf{G}|$ is small, the $T = 0$ transition is ultimately first order but a broad scaling regime exists [26, 27].

4.3 Spin charge separation in the $t-J$ model

A stronger violation of fermi liquid has been argued to occur in the two dimensional $t-J$ model believed to be relevant to high T_c superconductors. The fundamental idea, due to P W Anderson [28] and implemented in various different ways by P A Lee [29], A Larkin and others [30] is that 'spin charge separation' occurs, namely that the electron is very far from being an elementary excitation; instead the appropriate excitations are spinless charge carriers and neutral spin degrees of freedom. The most studied and the most promising version of this idea splits the electron into a charge e boson, b, and a neutral $S = 1/2$ fermion, f: $c^\dagger_{i\sigma} = b_i f^\dagger_{i\sigma}$. In this representation the states allowed in the $t-J$ model (in which doubly occupied states are excluded) are described as having one neutral fermion *or* one charged boson on each site, i.e. the constraint of no double occupancy becomes $b^\dagger_i b_i + f^\dagger_{i\sigma} f_{i\sigma} = 1$. The fermions are argued to fill a Fermi sea while the density of bosons is equal to the doping, i.e. the difference between the electron density and the density of the half filled band. If the bosons are condensed Fermi-liquid behavior is recovered with a quasiparticle weight of the order of the bose condensation amplitude; a strong non-Fermi-liquid is realized as long as the bosons do not condense. Bose condensation at $T = 0$ seems unavoidable in the models so far considered but it is possible that the bosons remain uncondensed over a wide and experimentally relevant temperature range. The bose condensation temperature can be made arbitrary small in the low doping limit (however a more quantitative study showed that it is unlikely that bosons remain uncondensed for parameters relevant to high T_c cuprates).

The separation of the electrons into bosons and fermions implies a local gauge invariance $b_i \to b_i \exp(i\phi)$, $f_i \to f_i \exp(i\phi)$; this leads to an internal gauge field which couples all the degrees of freedom. The screening of the gauge field by fermion particle-hole pairs leads to a gauge propagator of the form of Eqn (4) with $N = 2$. The effect of the gauge field on the bosons has also been considered in various analytical and numerical approximations. If the mass of the boson is larger than the mass of the fermion then a controlled perturbative expansion is possible which shows that the effect of the gauge field on the bosons is small [31]. In the opposite limit the analytical treatment shows that the bosons tend to phase separate into droplets [32] but the numerical treatment shows that there might exist a numerically large window with interesting properties [33].

4.4 Coupling to localized degrees of freedom and marginal Fermi liquid

An alternative route to non-Fermi-liquid behavior involves coupling a Fermi sea of electrons to a set of localized excitations. This issue arises in the context of heavy fermion materials which involve conduction electrons coupled to local moments [34]. This usually leads to a Fermi-liquid behavior but the possibility of non-Fermi-liquid behavior in some special cases is not ruled out. The issue also arises in the context of attempts to justify the 'marginal Fermi liquid' phenomenology [35] of high temperature superconductors. Briefly, the 'marginal Fermi liquid' assumes that a system of fermions retains its Luttinger Fermi surface but acquires a relaxation rate $\Gamma \propto \max(|\omega|, T)$ with a proportionality constant of the order of unity. Further, it is assumed that this relaxation rate is uniform around the Fermi surface and is due to the scattering by large angles and so determines the dc and optical conductivity. It was later realized that this ansatz does not provide an adequate description of the Hall angle or optical conductivity at intermediate frequencies but the concept remained and the interesting theoretical question of whether there is any fermion model in dimension $d > 1$ which displays this behavior remains open.

A large effort was invested in the construction of a model which exhibits such properties at least over a large frequency or temperature range but the results were mostly negative. Nevertheless it is not yet proven that such a model does not exist, moreover recent attempts based on the concept of Majorana local modes may eventually produce one.

Any self consistent model of a marginal Fermi liquid must be very different from the scattering by singular modes that were discussed in the previous sections because in all these models the scattering is due to soft bosonic modes which become soft at a particular point in the momentum space leading to predominantly forward scattering (as in the case of a quantum critical ferromagnet or gauge field) or to a large anisotropy around the Fermi surface (as in the case of a quantum critical antiferromagnet). Clearly this is not what one needs for the marginal Fermi liquid as defined above. Instead one would like to construct a model in which electrons scatter off of dispersionless entities with a propagator whose imaginary part is constant for $\omega > T$ and proportional to ω/T for $\omega < T$. The most promising proposed realization involves a localized (dispersionless) fermionic mode [36] which results, for example, in the scattering process shown in Fig. 5a. Evaluating this diagram gives

$$\Sigma(\omega) \sim \int G^2_{\rm el}(t, r = 0) G_{\rm f}(t) \exp(i\omega t)\, dt\,;$$

assuming that localized fermions have zero energy their Green function is $G_{\rm f}(t) = 1/t$ giving $\mathrm{Im}\Sigma(\omega) \propto \omega$ as required

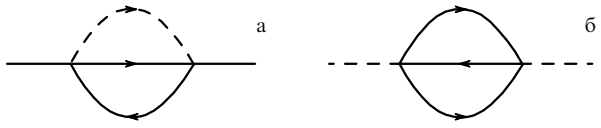

Figure 5. (a) Leading self energy correction to the itinerant electron Green function (solid line) due to scattering off of localized fermionic mode (dashed line). (b) Contribution to the self energy of the localized modes that generically moves them away from the Fermi surface and gives them dispersion.

for a marginal Fermi liquid.

The main difficulty with this model is that it is not self-consistent nor infra-red stable because in the same order of perturbation theory as that which gives the desirable $\Sigma(\omega)$ one also gets a contribution to the localized fermion energy shown in Fig. 5b which moves it away from the Fermi surface and gives it dispersion. These problems are avoided in by the models in which the energy shift is eliminated by fine tuning and which are further studied in the limit $d \to \infty$ which eliminates the dispersion [37]. An alternative approach involves representing the local degrees of freedom as real fermions such as introduced by Majorana in 1937. The idea is that normal fermions can be represented as a sum $\psi = \phi_1 + i\phi_2$ of two real fermionic fields; because $\phi^2 \equiv 0$, an action which depends only on one real Fermi field can not contain the term $E\phi^2$ and therefore such fermions always remain at the Fermi surface [38].

Real localized fermions are of course exotic objects but they do appear as a description of low energy excitations in at least one microscopic model, namely a two channel Kondo model which has electrons of two flavors interacting with a single spin $\sigma = 1/2$ impurity via the usual Kondo Hamiltonian

$$H_K = J \sum_{n=1,2} c^\dagger_{\alpha n} \boldsymbol{\sigma}_{\alpha\beta} c_{\beta n} \mathbf{S} . \tag{25}$$

The extra symmetry associated with the presence of two flavors of electrons guarantees that the energy shift vanishes. Unlike the usual Kondo problem this model does not have a qualitatively simple ground state because both the unscreened state (which can be regarded as a zeroth approximation at small J) and the overscreened state (which is a zeroth approximation at large J) are unstable. To construct the correct ground state and to explicitly observe the formation of the Majorana fermionic zero mode one performs a number of non-local operator transformations [38]. The crucial step is to note that charge and spin degrees of freedom are completely decoupled and have identical correlators in a non-interacting electron gas; so one can replace the spin interacting with two electron gases (25) by a spin interacting with spin and charge in the *same* electron gas

$$\widetilde{H}_K = J \sum (c^\dagger_\alpha \boldsymbol{\sigma}_{\alpha\beta} c_\beta + \tilde{c}^\dagger_\alpha \boldsymbol{\tau}_{\alpha\beta} \tilde{c}_\beta) \mathbf{S} , \tag{26}$$

where

$$\tilde{c} = \begin{pmatrix} c_\uparrow \\ c^\dagger_\downarrow \end{pmatrix}$$

is Nambu spinor and $\boldsymbol{\tau}$ isospin Pauli matrix associated with charge. The transformation from (25) to (26) is highly nonlocal from the view point of electron operators but the advantage of it is that now the interaction can be further rewritten as

$$\widetilde{H}_K = J(\phi_r \eta_r)^2 ,$$

where the ϕ_r are three (out of a total of four) real components of $c_\uparrow = 1/\sqrt{2}(\phi_1 - i\phi_2)$ and $c_\downarrow = -1/\sqrt{2}(\phi_3 + i\phi_0)$ operators and we have used the Majorana representation of spin $1/2$ operator $\mathbf{S} = \eta \times \eta$. In this final form one sees the appearance of the local Z_2 gauge invariance which a hybridization between spin and itinerant electrons would destroy. It is this local mode which is most adequately described by a Majorana fermion.

In this model there is no hybridization between the Majorana fermion and the conduction band, however the coupling between Majoranas on different sites via an intermediate state that contains three electrons generically will give them a dispersion thereby destroying the marginal Fermi liquid. However the energy scale at which dispersion becomes important has not yet been established for the two channel Kondo problem; it might be low because each Majorana fermion is coupled to three itinerant fermions that are related to electrons by a highly non-local transformation.

4.5 Pseudogap in high T_c cuprates

A different kind of non-Fermi-liquid behavior is displayed by underdoped high T_c cuprates. At high temperatures ($T > 200$ K) photoemission measurements of the electron Green function suggest that the materials have a large (Luttinger) Fermi surface [39] consistent with that predicted by band structure. As the temperature is lowered through a 'pseudogap scale' of order 200 K a gap opens up, eliminating parts of the Fermi surface near the momentum $(0, \pi)$ and $(\pi, 0)$ but leaving the parts near the zone diagonal $(\pi/2, \pi/2)$ unchanged. As T is decreased through the superconducting $T_c \sim 60 - 80$ K, the pseudogap evolves smoothly into $d_{x^2-y^2}$ superconducting gap.

This is non-Fermi-liquid behavior in the strong sense because it seems that parts of the Fermi surface are eliminated without the occurrence of long range order. It differs from the previously considered non-Fermi-liquid behaviors in that the density of states decreases rather than increases (e.g. the specific heat vanishes more rapidly than T). Theoretical explanations have involved incipient pairing [40–43] or antiferromagnetic [27, 44, 45] instabilities. The main unresolved issue is how to have fluctuations which are strong enough to produce a pseudogap without leading to long range order or at least to a correlation length with a very rapid temperature dependence.

5. Conclusion

For three and two dimensional clean materials a Fermi liquid is a surprisingly robust state of matter. On the theoretical side the only firmly established situations in which a clean material remains metallic but acquires a non-Fermi-liquid property are (i) proximity to a quantum critical point and (ii) the Halperin Lee and Read theory of a half-filled Landau level, these systems exhibit only 'weak non-Fermi-liquid' behavior. In $d = 2$ the theoretically predicted deviations from the conventional behavior are more pronounced and include a possible divergence of the staggered susceptibility at wave vector $Q = 2p_F$. The main problems presented by the experiment on clean materials are (i) critical behavior of metals near antiferromagnetic quantum critical point that disagrees with theoretical predictions and (ii) behavior of high T_c cuprates in optimally doped and underdoped regimes.

Acknowledgements. A J M thanks NSF-DMR-9707701 for support.

References

1. Devreese J T, Evrard R P, Van Doren V E (Eds) *Highly Conducting One-Dimensional Solids* (New York: Plenum Press, 1979)

2. Altshuler B L, Aronov A G, in *Electron-Electron Interactions in Disordered Systems* Ch. 1 (Modern Problems in Condensed Matter Sciences, Vol. 10, Eds A L Efros, M Pollak) (Amsterdam: North-Holland, 1985)
3. Prange R E, Girvin S M (Eds) *The Quantum Hall Effect* 2nd ed. (New York: Springer-Verlag, 1990)
4. "Proceedings of the Institute for Theoretical Physics Conference on Non-Fermi-Liquid Behaviour in Metals" *J. Phys. C* **8** 9675 (1996)
5. Abrikosov A A, Gorkov L P, Dzyaloshinski I E *Metody Kvantovoĭ Teorii Polya v Statisticheskoĭ Fizike'* (Methods of Quantum Fields Theory in Statistical Physics) (Moscow: Fizmatgiz, 1962) [Translated in English (Englewood Cliffs, NJ: Prentice-Hall, 1963)]
6. Shankar R *Rev. Mod. Phys.* **66** 129 (1994)
7. Anderson P W *Phys. Rev. Lett.* **71** 1220 (1993)
8. Yokoyama K, Fukuyama H *J. Phys. Soc. Jpn.* **66** 529 (1997)
9. Engelbrecht J R, Randeria M *Phys. Rev. B* **45** 12419 (1992)
10. Castellani C, Di Castro C, Metzner W *Phys. Rev. Lett.* **72** 316 (1994)
11. Pfleiderer C et al. *Phys. Rev.* **B 55** 8330 (1997)
12. Grosche F M et al. *Physica B* **206 – 207** 20 (1995)
13. Hertz J A *Phys. Rev. B* **14** 1165 (1976)
14. Millis A J *Phys. Rev. B* **48** 7183 (1993)
15. Belitz D, Kirkpatrick T R, Vojta T *Phys. Rev.* **B 55** 9452 (1997)
16. Altshuler B L, Ioffe L B, Millis A J *Phys. Rev. B* **50** 14048 (1994)
17. Khveshchenko D V *Phys. Rev.* **B 52** 4833 (1995); Khveshchenko D V, Stamp P C E *Phys. Rev.* **B 49** 5227 (1994)
18. Kwon H-J, Houghton A, Marston J B *Phys. Rev.* **B 52** 8002 (1995)
19. Holstein T, Norton R E, Pincus P *Phys. Rev.* **B 8** 2649 (1973)
20. Reizer M Yu *Phys. Rev. B* **40** (1989)
21. Halperin B I, Lee P A, Read N *Phys. Rev. B* **47** 7312 (1993)
22. Kalmeyer V, Zhang S -C *Phys. Rev. B* **46** 9889 (1992)
23. Migdal A A *Zh. Eksp. Teor. Fiz.* **32** 633 (1957) [*Sov. Phys. JETP* **5** 527 (1957)]
24. Hlubina R, Rice T M *Phys. Rev.* **B 51** 9253 (1995)
25. Julian S R *et al. J. Phys.* **C 8** 9675 (1996); von Lohneysen H *J. Phys.* **C 8** 9689 (1996) (Ref. [4])
26. Altshuler B L, Ioffe L B, Millis A J *Phys. Rev. B* **52** 5563 (1995)
27. Chubukov A V, Morr D K *Phys. Rep.* **288** 355 (1997)
28. Baskaran G, Zou Z, Anderson P W *Solid State Commun.* **63** 973 (1987)
29. Lee P A *Phys. Rev. Lett.* **63** 680 (1989)
30. Ioffe L B, Larkin A I *Phys. Rev. B* **39** 8988 (1989)
31. Ioffe L B, Kotliar G *Phys. Rev. B* **42** 10348 (1990)
32. Feigel'man M V et al. *Phys. Rev. B* **48** 16641 (1993)
33. Lee D K K, Kim H H, Lee P A *Phys. Rev. Lett.* **76** 4801 (1996)
34. Lee P A et al. *Comm. Cond. Matt. Phys.* **12** 99 (1986)
35. Varma C M et al. *Phys. Rev. Lett.* **63** 1996 (1989)
36. Ruckenstein A E, Varma C M *Physica C* **185–189** 134 (1991)
37. Si Q, Kotliar G *Phys. Rev.* **B 48** 13881 (1993)
38. Coleman P, Ioffe L B, Tsvelik A M *Phys. Rev. B* **52** 6611 (1995)
39. Shen Z-X, Dessau D S *Phys. Rep.* **253** 1 (1995)
40. Trivedi N, Randeria M *Phys. Rev. Lett.* **75** 312 (1995)
41. Altshuler B L, Ioffe L B, Millis A J *Phys. Rev. B* **53** 415 (1996)
42. Geshkenbein V B, Ioffe L B, Larkin A I *Phys. Rev. B* **55** 3173 (1997)
43. Emery V J, Kivelson S A *Nature* (London) **374** 434 (1995)
44. Vilk Y, Tremblay A M S *Europhys. Lett.* **33** 159 (1996)
45. Emery V J, Kivelson S A, Zachar O *Phys. Rev. B* **56** 6120 (1997)